



Numerical investigation of heat and mass transfer behavior of freeze drying of milk in vial

G. Srinivasan¹ · M. Muneeshwaran¹ · B. Raja¹

Received: 17 April 2018 / Accepted: 28 November 2018 / Published online: 11 January 2019
© Springer-Verlag GmbH Germany, part of Springer Nature 2019

Abstract

The transient heat and mass transfer characteristics of the freeze-drying process of milk in a vial is numerically investigated. The paper reports the influence of semi-stoppered vial on mass transfer resistance and the relative importance of the bottom curvature of the vial on the drying time. Moreover, the variation of product temperature and mass transfer resistance as a function of time is predicted. The study revealed that the vial heat transfer coefficient strongly depends on chamber pressure; however, the effect of shelf temperature is minimal. The analysis is conducted for two fill heights (8.25 and 16.5 mm.) It is observed that the presence of curvature at the bottom of the vial increases the primary drying time but decreases the product temperature. Based on the simulation, it is observed that 16.5 mm product fill height provided higher mass transfer resistance than 8.25 mm fill height.

Nomenclature

A_c	Contact area between vial and shelf, mm ²
c_p	Specific heat capacity, J kg ⁻¹ K ⁻¹
C_1	Empirical constant
h	Heat transfer coefficient, W m ⁻² K ⁻¹
$I(t)$	Sublimation interface position
k	Thermal conductivity, W m ⁻¹ K ⁻¹
k_c	Direct conduction heat transfer coefficient, W m ⁻² K ⁻¹
k_g	Gas conduction heat transfer coefficient, W m ⁻² K ⁻¹
k_v	Vial heat transfer coefficient, W m ⁻² K ⁻¹
l	Effective curvature depth, mm
L	Product height, mm
m	Sublimation rate, kg s ⁻¹
p_c	Chamber pressure, Pa
p_{eq}	Equilibrium vapor pressure of ice, Pa
p_v	Total pressure in the vial, Pa
q	Heat flux, W m ⁻²
R_d	Dry layer resistance, KPa s m ⁻² kg ⁻¹
R_s	Semi-stoppered vial resistance, KPa s m ⁻² kg ⁻¹
T	Temperature, K
t	Time, s
v_n	Normal velocity of sublimation interface, m s ⁻¹
z	Spatial coordinate

Greek symbols

ΔH_s	Sublimation enthalpy of ice, KJ kg ⁻¹
ρ	Density, kg m ⁻³
α	Thermal diffusivity, m ² s ⁻¹
α	Accommodation coefficient
λ_{amb}	Heat conductivity of water vapor at ambient pressure, W m ⁻¹ K ⁻¹
Λ	Free molecular heat conductivity of water vapor at 0 °C, W Pa ⁻¹ K ⁻¹ m ⁻²

Subscripts

f	Sublimation interface/front
g	Gas
s	Shelf
1	Dry layer
2	Frozen layer

1 Introduction

Freeze drying has been extensively used in the food and pharmaceutical industries for the manufacture of dried products, where the permitted residual moisture content is as low as 1 to 4% [1–3]. The process minimizes thermal degradation and especially, retains the original flavor and aroma in dried food products. A schematic representation of the freeze-drying process in a PT diagram and the variation of chamber pressure and product temperature is shown in Fig. 1a and b. The overall process contains three stages, namely freezing, primary drying, and secondary drying [1–4]. During freezing, the product to be dried is loaded on trays or into vials and mounted on a temperature-controlled shelves. The product is recommended to be

✉ B. Raja
rajab@iiitdm.c.in

¹ Indian Institute of Information Technology, Design and Manufacturing (IIITDM) Kancheepuram, Chennai, Tamil Nadu 600 127, India

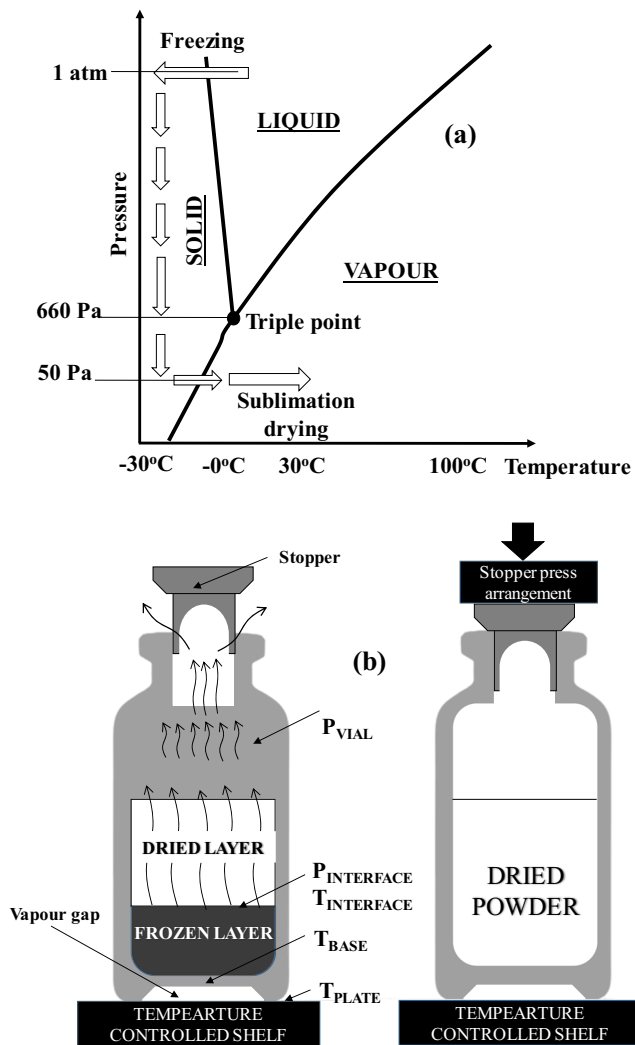


Fig. 1 a Schematic PT diagram b Glass vial arrangement on the shelf

frozen well below the eutectic temperature in the case of crystalline solutes and collapse temperature in the case of amorphous solutes. Freezing is followed by primary drying, where the frozen moisture content in the product is sublimated under vacuum. The chamber is recommended to be operated well below the triple point pressure of water to achieve an effective sublimation. In primary drying stage around 85 to 95% of the frozen water content is sublimated and the remaining is dehydrated by desorption in secondary drying stage. The primary drying stage consumes more time than the other two stages.

The overall process is influenced by (a) heat diffusion from the temperature-controlled shelves to the product, (b) the vacuum pressure difference between the region, where the product is loaded and the condenser, where the sublimated water vapor is condensed, (c) flow rate of the vacuum pump, (d) mass transfer resistance to the vapor flow. During vial freeze drying, the stopper is kept in a partially opened condition till the end of secondary drying and then

the stopper will be pushed into vial under vacuum. During this process the sublimated water vapor encounters three major flow resistance along its path from the product to the condensing chamber namely (1) resistance to water vapor flow due to the porosity in the dry layer (2) resistance due to the partially opened stopper (3) flow path resistance between the chamber and the condenser. The first resistance is attributed to Knudsen flow effect and the other two are attributed to both Knudsen and viscous flow effect. The contribution of the latter two resistances is less in comparison with the former, which is over 90% of the total flow resistance. Thermal diffusion resistance is caused in the contact between the vial and the shelf, where the curvature at the bottom of the vial entraps sublimated vapor. Pikal et al. [5] have demonstrated that the bottom curvature of the vial restricts the heat transfer to the product and causes a reduction in sublimation rate and increased drying time. Scutella et al. [6] have investigated the role of vial geometry on heat transfer coefficient and subsequently on product quality by predicting the product temperature distribution during the primary drying. King [7] proposed Uniformly Retreating Ice Front (URIF) model to a freeze-drying process and subsequently the same was improvised by Litchfield & Liapis [8] and Liapis & Marchello [9], which is commonly called as sorption-sublimation model. Mascarenhas et al., [10] presented a 2D axisymmetric finite element model for freeze drying process and computed a transient variation of the temperature, partial pressure of water vapor and the concentration of sorbed water and bound water in the dried layer. Sheehan and Liapis [11] studied the transient nature of vial freeze drying using the sorption-sublimation model. Hottot et al., [12] performed simulation to study the temperature pattern and sublimation front velocities of bovine serum albumin using 2D axisymmetric model and reported that the heat transfer from shelf and surrounding to the product controls the sublimation process. Song et al. [13] developed a moving boundary model and conducted detailed experiments on skimmed milk and explored a multi-dimensional characteristic of the vial freeze-drying process. In this study, a dynamic two-dimensional numerical analysis is carried out for primary drying stage using COMSOL Multiphysics software. A vial of 15 mm in diameter with a milk of 16.5 and 8.25 mm fill height is considered for analysis and the numerical result is validated with the available results in the published literature of Mascarenhas et al., [10]. The curvature at the bottom of the vial is considered to find its influence on the drying process parameters such as product temperature and drying time. The objectives of the work are (a) to simulate a vial freeze drying process and predict the heat and mass transfer behavior (b) to study the chamber pressure influence on overall heat transfer coefficient (c) to find the effect of bottom curvature of vial

on the heat and mass transfer behavior using the method proposed by Scutella et al. [6].

2 Governing equation

The region of interest and the corresponding boundary conditions are shown in Fig. 2. The region is demarcated into two parts and termed as dried and frozen region. During sublimation, the interface moves towards the bottom of vial and in turn increases the thickness of dry layer, which is formed above the interface. The primary drying process ends when the sublimation interface reaches the bottom of the vial. The term q represents the heat flux supplied to the vial from shelf. The radiation heat transfer through the sides of the vial is neglected in this study. The following are the assumptions made in this study (a) One dimensional heat and mass transfer along the axis of the vial, (b) The sublimation front is in thermodynamic equilibrium with the sublimated water vapor, (c) the sublimation interface has negligible thickness, (d) uniform thermo-physical properties of both frozen and dry material, (e) No shrinkage in the dried cake. Temperature distribution in the dried and frozen region is described in the following equations.

$$\frac{\partial T_1}{\partial t} = \alpha_1 \frac{\partial^2 T_1}{\partial z^2} \quad (1)$$

$$\frac{\partial T_2}{\partial t} = \alpha_2 \frac{\partial^2 T_2}{\partial z^2} \quad (2)$$

Where, $\alpha_1 = k_1/\rho_1 C_{p1}$, $\alpha_2 = k_2/\rho_2 C_{p2}$, the spatial domain for dry region is $0 \leq z \leq I(t)$, while for frozen region is $I(t) \leq z \leq L$.

The boundary conditions are,

$$At z = 0, \quad q = h^*(T - T_1) \quad (3)$$

$$At z = I(t), \quad T_1 = T_f \quad (4)$$

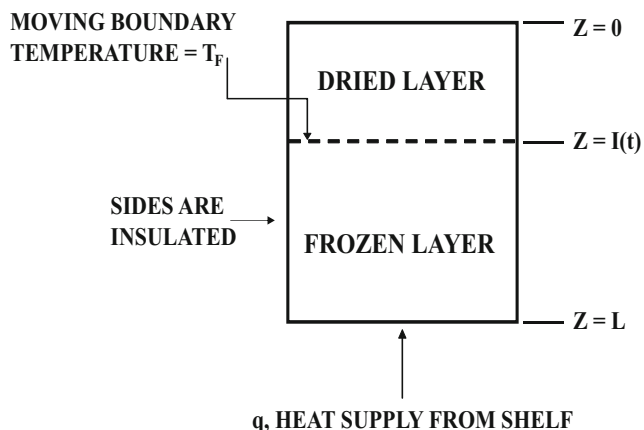


Fig. 2 Domain of interest

$$At z = I(t), \quad T_2 = T_f \quad (5)$$

The sublimation front temperature (T_f) is a process variable. It can be computed as a function of equilibrium pressure of water vapor at sublimation interface, using Clausius-Clapeyron relation [9].

$$T_f = \frac{6139.6}{28.8912 - \ln(P_{eq})} \quad (6)$$

The equilibrium vapor pressure of ice can be estimated by using the following equation [14].

$$P_{eq} = \exp\left(9.550426 - \frac{5723.26}{T} + 3.53068 \ln(T) - 0.00728332 T\right) \quad (7)$$

A two-dimensional finite element numerical model and with an arbitrary Lagrangian-Eulerian (ALE) scheme for tracking the sublimation front is used throughout the simulation. This time dependent study is solved using Multifrontal Massively Parallel Sparse direct solver (MUMPS) with the time steps of 100 s. The Backward differentiation formula (BDF) time stepping method is employed with the maximum order of 2. The relative tolerance of $1e^{-20}$ is taken to get an accurate result.

2.1 Grid independence test

To check the influence of the grid size on the numerical results, a case with a fill height of 8.25 mm (without considering the curvature effect) is simulated for normal, fine, finer and extra fine grids involving 224, 360, 700 and 2346 structured quadrilateral elements respectively. The results of the grid independence study are listed in Table 1. Compared to the reference results (that on the extra fine), the obtained primary drying time for normal grid shows a relative error of 0.5%, this difference is still too large for accurate simulation. On the other hand, the finer grid leads to a relative error of 0.241% compared to the reference, which is acceptable, and the same mesh pattern has been retained for the remaining simulations.

Table 1 Grid independence study result

Mesh type	No of quadrilateral elements	Relative error (%)
Normal	224	0.5
Fine	360	0.304
Finer	700	0.241
Extra fine	2346	Reference

3 Results and discussion

A time dependent and 2-D axisymmetric finite element simulation of the sublimation dehydration of milk in a vial is performed using COMSOL Multiphysics. The model mimics a vial with inner radius of 7.5 mm and different fill heights of 16.5 and 8.25 mm. The material properties and other parameters used for this study are listed in Table 2. As an initialization guess, the interface position is assumed to be at a location of 0.1 mm from the top surface. As the drying simulation progresses, the interface tends to recede towards the bottom of vial by reconstituting the mesh. The solution is obtained by coupling the heat transfer and deformed geometry module in the software.

3.1 Validation of the model

This section presents the validation of our model against the published literature. The parameters like temperature profile, sublimation interface position and variation of vial heat transfer coefficient (k_v) with respect to chamber pressure are validated with literatures [6, 10].

Mascarenhas et al., [10] did a numerical analysis of freeze drying of bovine somatotropin (BST). The properties of skimmed milk and BST are similar and hence skimmed milk values are used by the author [10]. The test conditions taken in our work is identical to Mascarenhas et al., [10]. The parameters like temperature profile, sublimation interface position

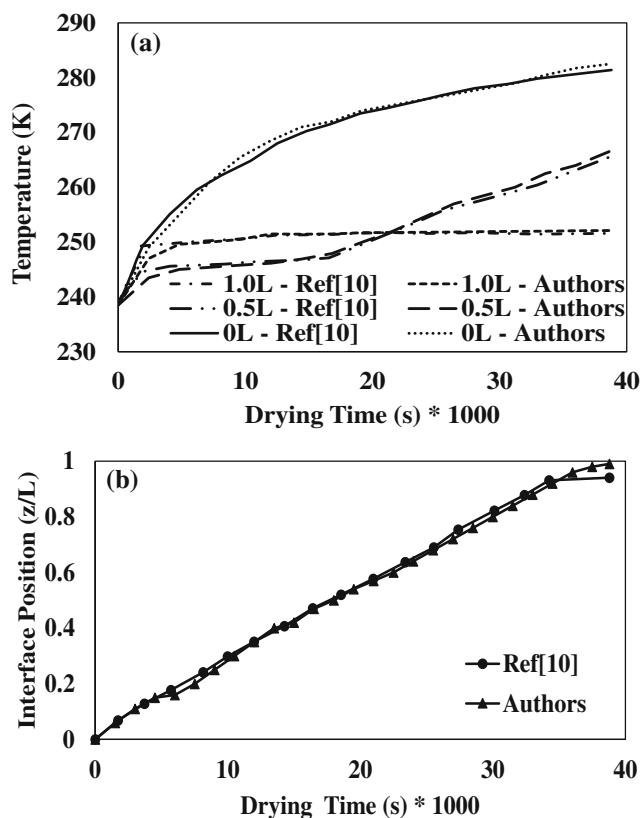


Fig. 3 Validation against literature [10] a Temperature history b Position of sublimation interface

are compared with the literature [10] as shown in Fig. 3a and b and a good agreement is seen.

Table 2 Material properties and input data

Parameter	Symbol	Value	Unit
Density - dry layer	ρ_1	145 [13]	kg/m ³
Density - frozen layer	ρ_2	1050 [13]	kg/m ³
Specific heat - dry layer	C_{p1}	2590 [13]	J/(kg*K)
Specific heat - frozen layer	C_{p2}	1930 [13]	J/(kg*K)
Thermal conductivity - dry layer	k_1	0.01 [13]	W/(m*K)
Thermal conductivity -frozen layer	k_2	2.1 [13]	W/(m*K)
Initial temperature	T_{init}	248.8	K
Shelf temperature	T_s	263.15	K
Latent heat of Sublimation	ΔH_s	2840	KJ/kg
Chamber pressure	p_c	10–100	Pa
Shelf heat transfer coefficient	h_c	90	W/(m ² *K)
Outer bottom area of the vial	A_o	$2.07 \cdot 10^{-4}$ [6]	m ²
Inner bottom area of the vial	A_i	$1.78 \cdot 10^{-4}$ [6]	m ²
Vial-shelf contact area	A_c	$1.67 \cdot 10^{-5}$ [6]	m ²
Mean bottom curvature depth	l	$1.23 \cdot 10^{-4}$ [6]	m
Molecular conductivity of the water vapor at ambient pressure	λ_{amb}	0.025 [6]	W/(m*K)
Free molecular flow heat transfer coefficient	Λ	1.99 [6]	W/(Pa*K*m ²)
Accommodation coefficient (water vapor)	α	0.48 [6]	Dimensionless
Heat transfer model coefficient	C_1	$2.15 \cdot 10^5$ [6]	W/(m ⁴ *K)

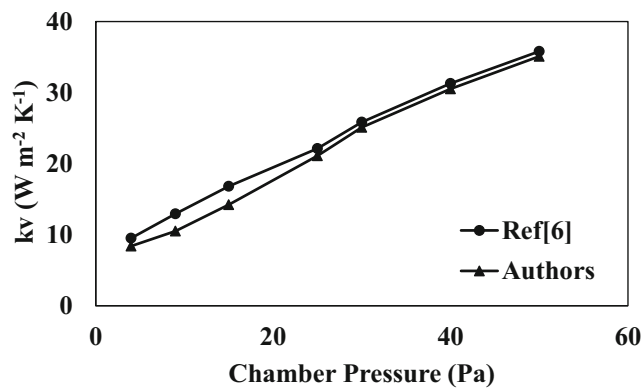


Fig. 4 Validation of vial heat transfer coefficient (K_v) against literature [6]

The variation of vial heat transfer coefficient (k_v) with respect to chamber pressure is validated by comparing with the work of Scutella et al., [6]. Scutella et al. studied the effect of the contact area between vial and shelf on various ranges of chamber pressure (4 to 50 Pascal) and shelf temperature (-40 to 0 °C). As observed in Fig. 4, a good agreement between our work and literature [6] is observed at chamber pressure values between 20 and 50. However, at low chamber pressures, the variation in vial heat transfer coefficient (k_v) is attributed due to the exclusion of radiative effects in the present study.

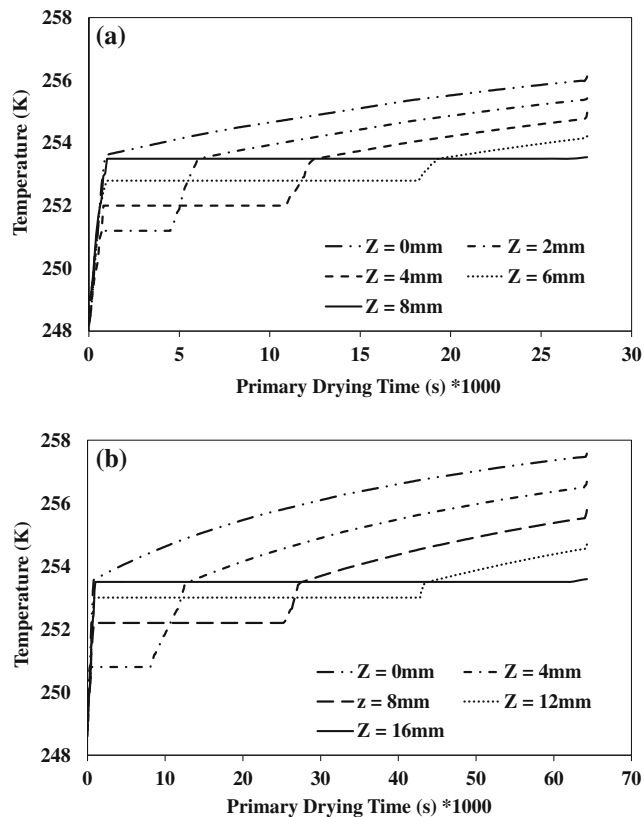


Fig. 5 Temperature history of Milk during primary drying stage of freeze drying – Without considering the vial curvature effect a 8.25 mm fill height b 16.5 mm fill height

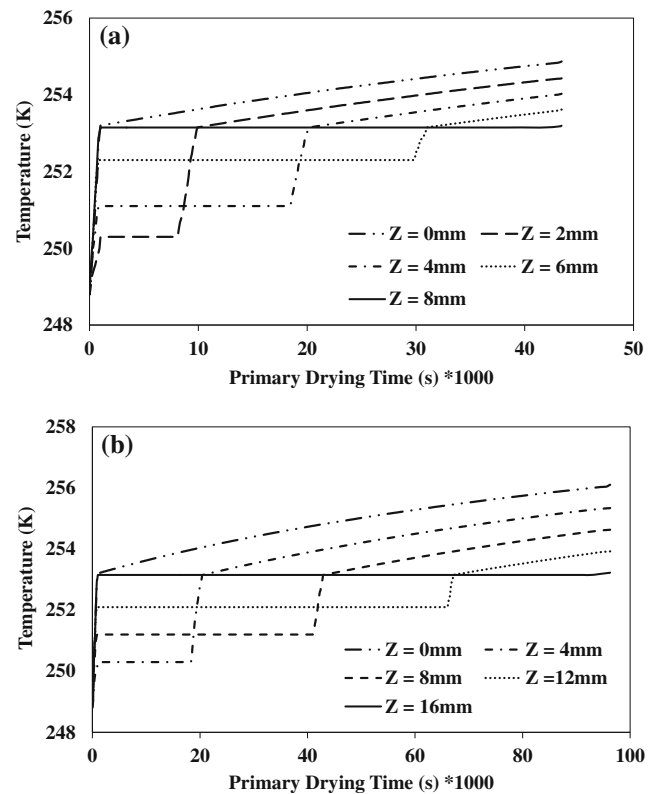


Fig. 6 Temperature history of Milk during primary drying stage of freeze drying – With considering the vial curvature effect a 8.25 mm fill height b 16.5 mm fill height

3.2 Temperature history

The time-temperature plot at a chamber pressure of 100 Pa corresponding to five different depths from the top surface is shown in Fig. 5 (without the effect of bottom curvature) and Fig. 6 (with the effect of bottom curvature). The temperature in the frozen region is observed to be almost constant (with only slight variation), but in the dry region the same tend to exhibit a steep slope. This is due to the supplied heat to ice layer is utilized for latent heat of sublimation of ice, which resulted in a constant temperature. However, in the dry region the energy is used to increase the sensible heat of the product and resulted a steep temperature gradient. The fill height of the product in a vial plays an important role and influence both the product temperature and drying time. For instance, the model with 8.25 mm fill height experienced a low temperature than one with 16.5 mm fill height. Irrespective of the curvature effect, milk with 8.25 mm fill height tend to experience around 1.2 – 1.5 °C lesser than the one with 16.5 mm fill height.

For the simulated condition, the maximum temperature attained depends on fill heights. For the 8.25 mm fill height, the maximum temperature attained without and with considering the curvature effect is 256.1 and 254.9 °C respectively. Whereas, the same for 16.5 mm fill height is predicted as

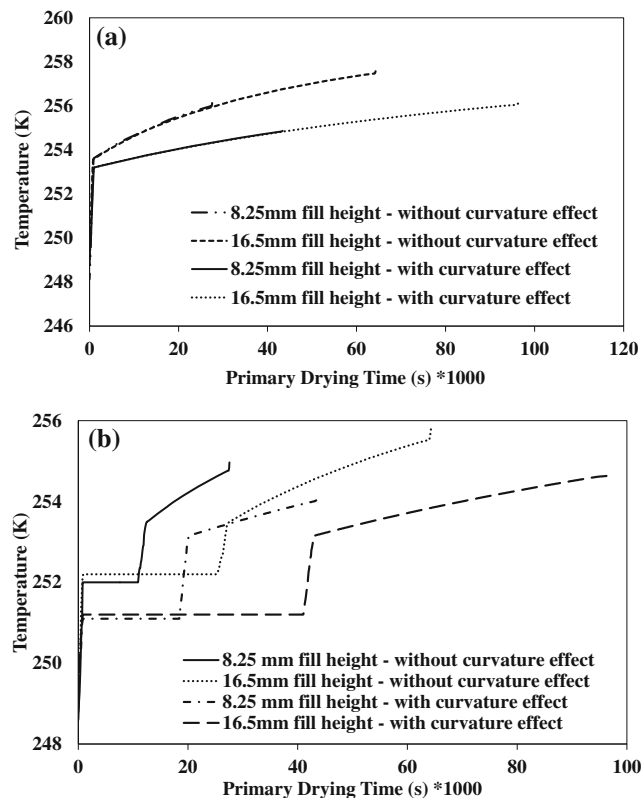


Fig. 7 Temperature versus Drying Time **a** at 0 L **b** at 0.5 L

257.6 and 256.1 °C respectively. The temperature variation at the top surface and 0.5 L is shown in Fig. 7. It is observed from Fig. 7a that the trend of temperature variation is different for without and with considering the curvature effect. However, in both the cases the temperature variation trend is same irrespective of the fill height. This is only valid in the region very close to the top surface, whereas the same varies for the layers away from the top, which is shown in Fig. 7b.

3.3 Position of sublimation of interface

As the sublimation front recedes, it is necessary to impose moving boundary condition on the interface. The velocity of the sublimation interface is attained by a heat balance at the sublimation front. The heat flux from the dry region entering the sublimation interface is equal to the sum of heat flux from frozen region plus the heat absorbed at the interface due to sublimation. This heat balance gives Stefan equation [10, 15] and the velocity of the sublimation interface can be estimated using $V_n = (q_2 - q_1) / (\rho_2 - \rho_1) \Delta H_s$. The sublimation interface position against drying time at a chamber pressure of 100 Pa predicted using Arbitrary Lagrangian-Eulerian (ALE) is shown in Fig. 8a and b, where the z-axis is normalized with respect to the thickness of the product. The moving boundary contour captured during the simulation is shown in Fig. 9. Though, experimental prediction of exact location of sublimation interface is a difficult task, the same could be tracked by

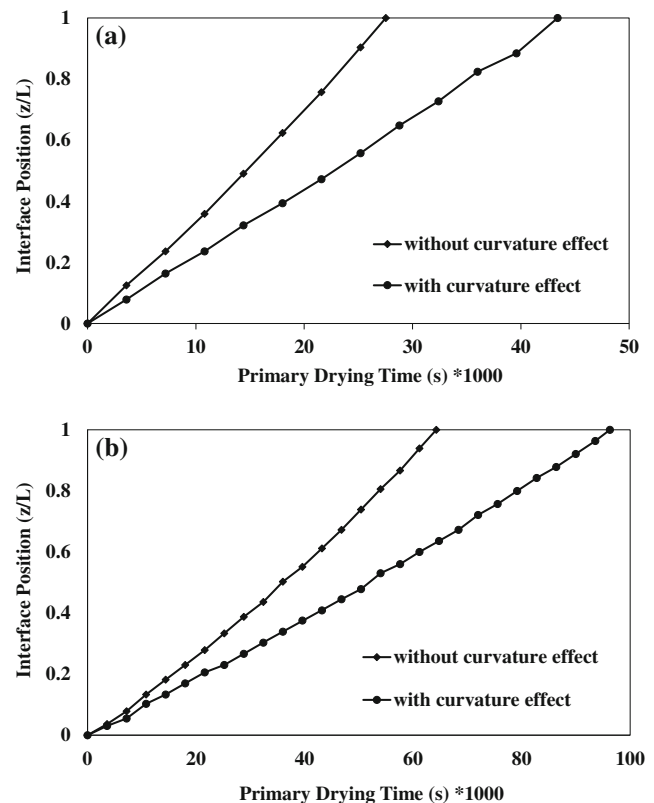


Fig. 8 Sublimation interface location versus primary drying time – **a** 8.25 mm fill height **b** 16.5 mm fill height

numerical analysis easily. The interface position and thus the drying time directly depends on the fill height of the sample in the vial. For the case without considering the curvature effect, sublimation interface velocity for 8.25 and 16.25 mm fill heights are 0.299 and 0.256 $\mu\text{m/s}$ respectively. Upon considering the curvature effect, the sublimation interface velocity reduces to 0.19 and 0.17 $\mu\text{m/s}$ respectively for 8.25 and 16.5 mm fill heights. It is observed that the interface velocity and the dried layer mass transfer resistance depends on the fill height. The former and the latter are inversely and directly proportional to the fill height respectively. In case of 8.25 mm fill height, the computed primary drying time by considering the effect of bottom curvature of vial is almost 4.4 h higher than the one without considering the effect of bottom curvature of vial. Similarly, for 16.5 mm fill height the difference in primary drying is observed to be 8.9 h. This is due to the heat transfer resistance rendered by the vapor entrapped between vial and shelf.

3.4 Mass transfer resistance

In the dry region, the mean free path of water vapor is large compared with pore dimension, hence flow in dry region is free molecular or Knudsen flow which is driven by pressure difference between equilibrium vapor pressure of ice and partial pressure of water vapor above the dried product [5]. So,

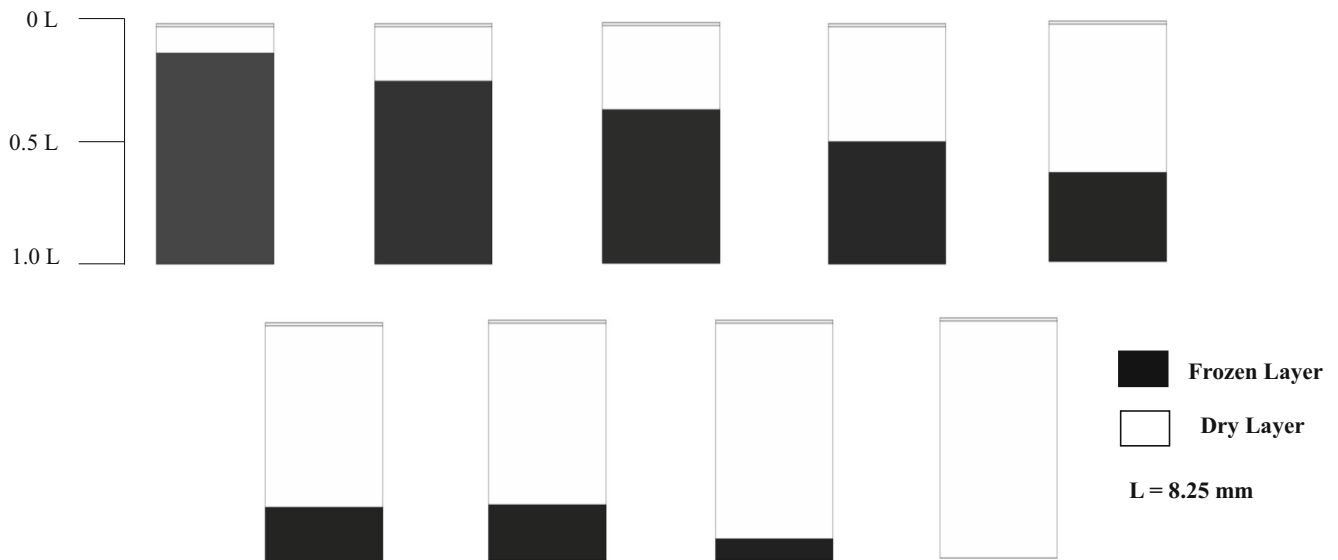


Fig. 9 Position of Sublimation interface predicted by COMSOL Multiphysics at the interval of 1 h – 8.25 mm fill height (without considering the effect of curvature)

the dry layer resistance to water vapor flow can be expressed as $R_d = (p_{eq} - p_v) / \dot{m}$. The mean free path of water vapor is smaller in the vial and chamber, so the flow is predominantly viscous flow. The difference between total pressure in vial and chamber can be taken as a driving force. The resistance of the

semi-stoppered vial can be defined as $R_s = (p_v - p_c) / \dot{m}$. The resistance offered by chamber – condenser pathway is neglected in this study. The dry layer resistance versus primary drying time at a chamber pressure of 100 Pa is shown in Fig. 10. At the incipience of drying, the sublimation interface starts to move from the top layer to the bottom of the vial and it

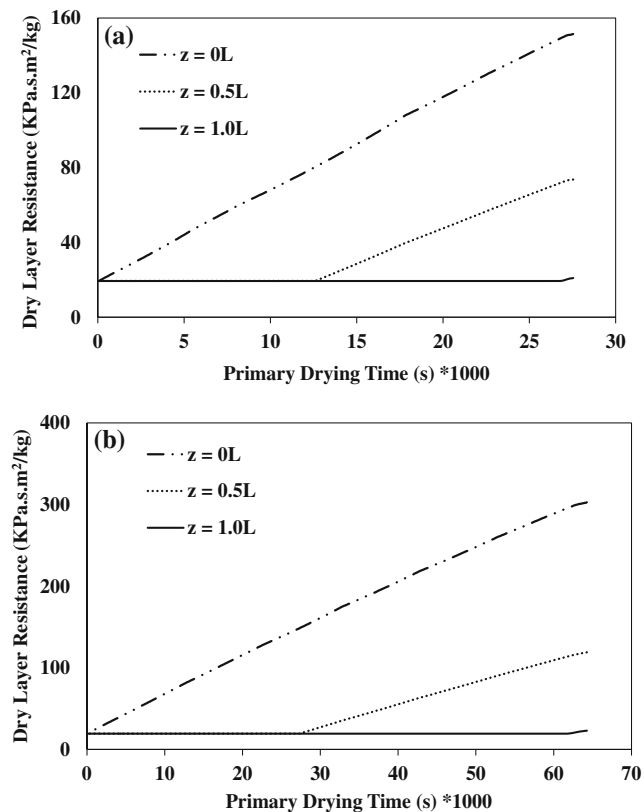


Fig. 10 Dry Layer Resistance versus primary Drying Time – a 8.25 mm fill height b 16.5 mm fill height

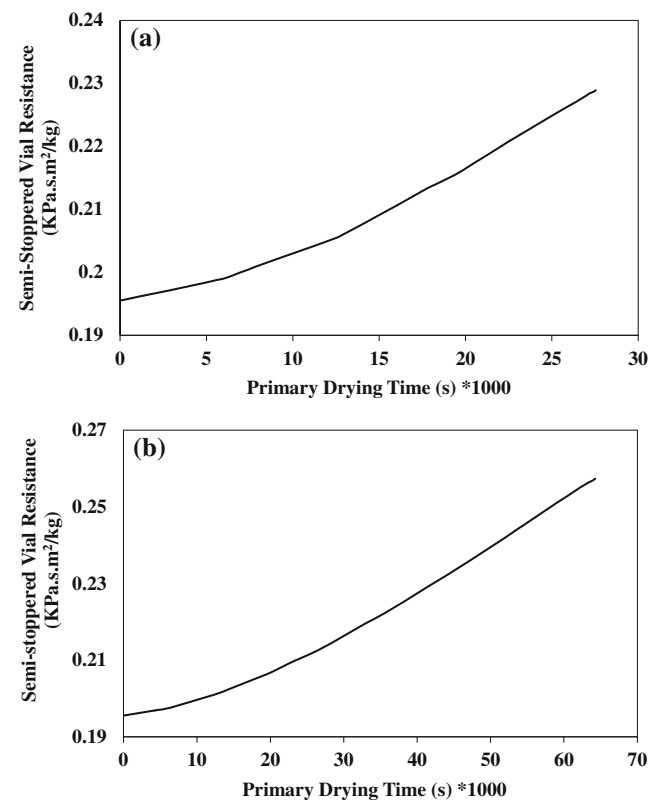


Fig. 11 Semi stoppered vial Resistance versus primary Drying Time – a 8.25 mm fill height b 16.5 mm fill height

leaves the dry layer above the interface. As the drying progresses the thickness of the dry layer grows gradually and in turn increases the mass transfer resistance to water vapor flow. The maximum dry layer resistance for 8.25 and 16.5 mm fill heights of milk is 152 and 303 kPa.s.m.²/kg respectively.

The resistance offered by the semi-stoppered vial at a chamber pressure of 100 Pa is shown in Fig. 11. The effective diameter of closure taken for computing the area normalized semi-stoppered resistance is 4 mm. The maximum semi-stoppered vial resistance for 8.25 and 16.5 mm fill heights is 0.228 and 0.257 kPa.s.m.²/kg respectively. From the analyses, it is observed that the resistance offered by the dry layer contributes more than 95% of total resistance, whereas the semi-stoppered vial resistance is less than 1 to 2% only. In dry region, mean free path of water vapor is larger than the pore size, hence it acts as a main hindrance to the flow of water vapor. Even though, the semi-stoppered vial resistance is very minimum when compared to the dry layer resistance, it could be further reduced by positioning the closure in such a way that it configures more effective diameter.

3.5 Impact of chamber pressure on k_v and drying time

The vial heat transfer coefficient (k_v) is the sum of heat transfer coefficient due to direct contact (k_c), gas conduction (k_g) and radiation (k_r) ($k_v = k_c + k_g + k_r$). The direct contact conduction is discussed by Kuu et al., [16] which is a function of direct contact area between shelf and vial. It can be stated that the higher contact area between shelf and vial will result in a large contact conduction heat transfer coefficient, $k_c = C_1 A_c$. It is explained earlier that due to curvature at the bottom, the vial is partially in direct contact with the shelf. A significant portion of the bottom part of the vial traps gas, which acts as a heat transfer barrier between shelf and the vial surface. The coefficient k_g , represents the vapour (trapped between vial and shelf) conduction heat transfer coefficient. Using Smoluchowski theory [6] and characterizing the distance between vial bottom and shelf by 'l', the gas conduction heat transfer coefficient can be expressed as $k_g = C_2 p_c / (1 + (l C_2 p_c / \lambda_{amb}))$, where $C_2 = (\Lambda \alpha / 2 - \alpha) 16.52 T_g^{-0.5}$. This gas conduction heat transfer coefficient increases with chamber pressure. But for a better sublimation, the chamber pressure is always kept as a constant and as low as possible. The radiative heat transfer is not considered in this study.

The chamber pressure influence on the vial heat transfer coefficient is studied for the pressure range between 10 and 100 Pa. The variation of vial heat transfer coefficient against chamber pressure for the shelf temperature of 263 K is shown in Fig. 12. As the chamber pressure increases, the value of k_g increases and the vial heat transfer coefficient at a chamber pressure of 100 Pa is approximately 5 times higher than the value at 10 Pa. This prediction agrees well with the results published in Scutella et al. [6]. The variation trend of vial heat

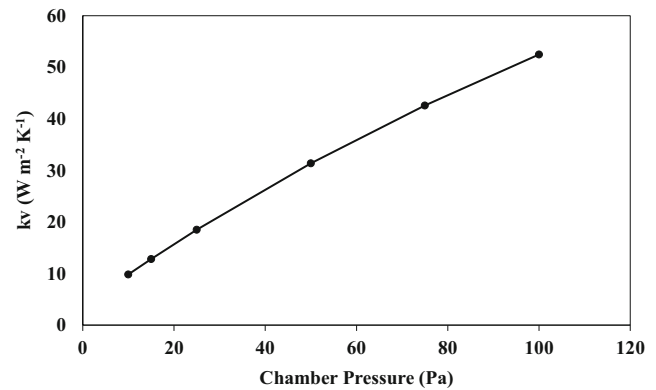


Fig. 12 Vial heat transfer coefficient versus Chamber Pressure for the shelf temperature of 263 K

transfer coefficient with chamber pressure is similar for both 8.25 and 16.5 mm fill height. The relative contribution of k_c and k_g on total k_v is shown in Fig. 13. At low pressure range, say between 10 and 15 Pa, the contribution of k_c is almost in the range of 28 to 36%, whereas at higher pressure range, the same reduces to 7%. The contribution of gas conduction heat transfer coefficient (k_g) is 63% at 10 Pa and 93% at 100 Pa. This indicates that the gas conduction heat transfer coefficient is a strong function of chamber pressure. From Fig. 13, it can be observed that the difference between the relative importance of k_g on total k_v at 75 Pa and 100 Pa is 1% only. To evaluate the influence of shelf temperature on total k_v , the analyses was carried out for the various shelf temperatures of 263, 273 and 283 K, and at the pressure range from 10 to 100 Pa. The study revealed no significant variation of k_v with respect to the shelf temperature. The variation of drying time with respect to chamber pressure is shown in Fig. 14. The reduction in drying time is observed at higher chamber pressure levels. This is due to the attainment of higher vial heat transfer coefficient values at higher pressure range.

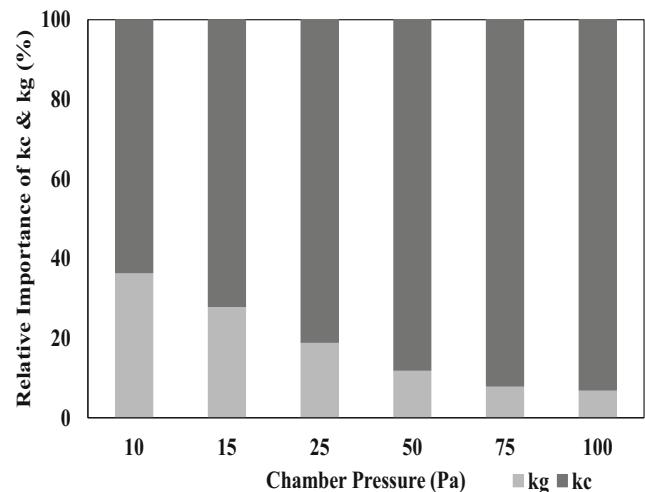


Fig. 13 Relative contribution of k_c and k_g on total k_v versus Chamber Pressure

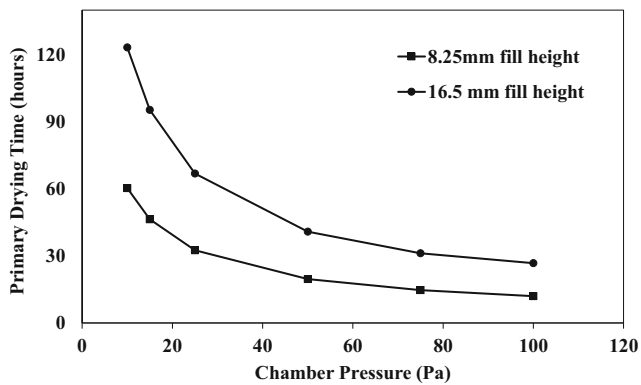


Fig. 14 Drying time versus Chamber Pressure

4 Conclusions

A finite element simulation of freeze-drying of milk in a vial is carried out for different fill heights. The results showed that the vial geometry plays a vital role in determining the freeze drying parameters such as product temperature, drying time. The effect of chamber pressure on the gas conduction and overall vial heat transfer coefficient is also studied. The following are the main observation of this study.

- The product temperature and drying time depends on the fill height. For instance, at a chamber pressure of 100 Pa and without the curvature effect, the milk with fill height of 8.25 mm experienced 1.2 to 1.5 °C less than the one with 16.5 mm. The drying time of 8.25 mm fill height is 4.4 h lesser than 16.5 mm fill height.
- The sublimation interface velocity depends on the product fill height and the bottom curvature of the vial. For the case without considering the curvature effect, the sublimation front velocity is observed respectively to be 0.299 and 0.256 $\mu\text{m/s}$ for 8.25 and 16.5 mm fill heights. The same reduces to 0.19 and 0.17 $\mu\text{m/s}$ if the curvature effects are considered.
- Dry layer mass transfer resistance accounts more than 95% of total resistance, and whereas the semi-stoppered vial resistance is less than 1–2%.
- With reference to the simulated conditions, the vial heat transfer coefficient strongly depends on chamber pressure and weakly on shelf temperature. For instance, the coefficient at 100 Pa is approximately 5 times higher than the value at 10 Pa. The vial heat transfer coefficient is also observed to be independent of the fill height.
- The gas conduction heat transfer coefficient is a strong function of chamber pressure and dominant component in the total heat transfer coefficient at a higher chamber pressure only.

Acknowledgements The authors would like to thank Department of Science and Technology (DST-SERC), India (Ref no: SR/S3/MMER/

0005/2014) for their financial aid to carry out the work and Dr. Joseph Daniel of VIT Chennai for extending COMSOL license.

Compliance with ethical standards

Conflict of interest We have no potential conflict of interest to declare.

Publisher's Note Springer Nature remains neutral with regard to jurisdictional claims in published maps and institutional affiliations.

References

1. Kremer DM, Pikal MJ, Petre WJ, Shalaev EY, Gatlin LA, Kramer T (2009) A procedure to optimize scale-up for the primary drying phase of lyophilization. *J Pharm Sci* 98:307–318
2. Ebubekir SA, Ozgun Y, Hasan S (2017) Modelling and simulation of a moving interface problem: freeze drying of black tea extract. *Heat Mass Transf* 53:2143–2154
3. Scutella B, Plana-Fattori A, Passot S, Bourles E, Fonseca F, Flick D, Trelea IC (2017) 3D mathematical modelling to understand a typical heat transfer observed in vial freeze drying. *Appl Therm Eng* 126:226–236
4. Millman MJ, Liapsis AI, Marchello JM (1984) Guidelines for the desirable operation of batch freeze driers during the removal of free water. *Int J Food Sci Technol* 19:725–738
5. Pikal MJ, Roy ML, Shah S (1983) Mass and heat transfer in vial freeze-drying of pharmaceuticals: role of the vial. *J Pharm Sci* 73: 1224–1237
6. Scutella B, Passot S, Bourles E, Fonseca F, Trelea IC (2016) How vial geometry influences heat transfer and product temperature during freeze drying. *J Pharm Sci* 106:770–778
7. King CJ (1971) *Drying of foods*. CRC Press, Cleveland, pp 1–54
8. Litchfield RJ, Liapsis AI (1979) An adsorption-sublimation model for a freeze dryer. *Chem Eng Sci* 34:1085–1090
9. Liapsis AI, Marchello JM (1984) Advances in the modelling and control of freeze drying. In: Mujumdar AS (ed) *Advances in drying*, vol 3. Hemisphere Publishing Corporation, Washington, DC, pp 217–244
10. Mascarenhas WJ, Akay HU, Pikal MJ (1997) A computational model for finite element analysis of the freeze-drying process. *Comput Methods Appl Mech Eng* 148:105–124
11. Sheehan P, Liapsis AI (1998) Modeling of the primary and secondary drying stages of the freeze drying of pharmaceutical products in containers: numerical results obtained from the solution of a dynamic and spatially multi-dimensional lyophilization model for different operational policies. *Biotechnol Bioeng* 60:712–728
12. Hottot PR, Vessot S, Andrieu J (2006) Freeze drying of pharmaceutical proteins in vials: modeling of freezing and sublimation steps. *Dry Technol* 24:561–570
13. Song CS, Nam JH, Kim CJ, Ro ST (2005) Temperature distribution in a vial during freeze-drying of skim Milk. *J Food Eng* 67:467–475
14. Warning AD, Arquiza JMR, Datta AK (2014) A multiphase porous medium distributed sublimation front to simulate vacuum freeze drying. *Food Bioprod Process* 94:637–648
15. Bogdani E, Vessot S, Andrieu J (2013) Experimental and modeling study during freeze-drying of aqueous tert-butanol based formulation in vials. *Dry Technol* 31:1772–1779
16. Kuu WY, Nail SL, Sacha G (2009) Rapid determination of vial heat transfer parameters using tunable diode laser absorption spectroscopy in response to step changes in pressure set point during freeze drying. *J Pharm Sci* 98:1136–1154